Pressure-induced superconductivity in trigonal layered math xmlns="http://www.w3.org/1998/Math/MathML">msub>mi>PtBi/mi>mn>2/mn>/msub>/math> with triply degenerate point fermions

Jing Wang, Xuliang Chen, Yonghui Zhou, Chao An, Ying Zhou, Chuanchuan Gu, Mingliang Tian, and Zhaorong Yang

Phys. Rev. B **103**, 014507 — Published 11 January 2021

DOI: 10.1103/PhysRevB.103.014507

Pressure-induced superconductivity in trigonal layered $PtBi_2$ with triply degenerate point fermions

Jing Wang,[1,2] Xuliang Chen,[1,3,*] Yonghui Zhou,[1,3] Chao An,[4] Ying Zhou,[4] Chuanchuan Gu,[5] Mingliang Tian,[1,3] and Zhaorong Yang[1,3,4,†]

[1]*Anhui Province Key Laboratory of Condensed Matter Physics at Extreme Conditions, High Magnetic Field Laboratory, Chinese Academy of Sciences, Hefei 230031, China*
[2]*Science Island Branch of Graduate School, University of Science and Technology of China, Hefei 230026, China*
[3]*High Magnetic Field Laboratory of Anhui Province, Hefei 230031, China*
[4]*Institutes of Physical Science and Information Technology, Anhui University, Hefei 230601, China*
[5]*Department of Materials Science and Engineering, Southern University of Science and Technology, Shenzhen 518055, China*

(Dated: November 27, 2020)

Materials with non-saturating, extremely large magnetoresistance (XMR) attract continuous research interest due to their great potentials in the fields of spintronics and magnetic sensors/switchs. Here, we report the discovery of pressure-driven superconductivity (SC) in trigonal $PtBi_2$, a semimetal material with nontrivial triply degenerate point fermions exhibiting non-saturating XMR effect, above a critical pressure of ∼5-6 GPa. The superconducting transition onset temperature is ∼2 K and displays a very weak pressure dependence across a broad pressure range of ∼5-48 GPa. The lattice structure of trigonal $PtBi_2$ is stable against pressure at least to 12.9 GPa. Around the same critical pressure where the SC emerges, the Hall coefficient varies violently and shows a sign crossover from low-pressure positive (hole-dominated) to high-pressure negative (electron-dominated), probably indicating a close relationship between them.

I. INTRODUCTION

Pressure, as one of the fundamental thermodynamic parameters, plays a significant and indispensible role on the study of superconductivity (SC). It can drive a material that is not superconductive at ambient pressure into a superconductor and/or modify the superconducting phase transition temperature (T_C) effectively. Typical examples include inducing SCs in BCS-type non-superconducting elements[1,2] and poly-H systems like S-H[3] and La-H[4] (where to date a record high T_C of ∼ 260 K has been achieved). Intuitively, SCs in these materials under high pressure are made possible owing to enrichment of the carriers concentration and/or enhancement of the electron-phonon coupling. In addition, pressure can optimize or introduce SCs in many unconventional systems[5,6] like heavy-fermion materials, cuprates or iron-based compounds, by suppressing some orders to zero temperature and realizing a quantum critical point.

Over the past decade, materials with non-saturating, extremely large magnetoresistance (XMR) attracted continuous research interest due to their great potentials in the fields of spintronics and magnetic sensors/switchs. Empirically, one may find that applying pressure to these materials can suppress their XMR and induce SC. Indeed, there have been many reports on pressure-induced SC in the XMR materials, such as (W/Mo)Te_2,[7–9] (Zr/Hf)Te_5,[10–12] Cd_3As_2,[13] and so on. Usually, these XMR materials, referred to as topological electronic materials (new quantum states of matter), have non-trivial bulk or surface band structures featuring in linear dispersions in the momentum space. In addition to the XMR, these materials manifest ultrahigh carriers mobility and low carriers density.[14,15] Since these XMR semimetals generally have relatively low carrier density ($\sim 10^{18-20}/\mathrm{cm}^3$)[14,15] than that of conventional metals ($\sim 10^{22}/\mathrm{cm}^3$), application of pressure may lead to a rapid enhancement in carriers density due to shrinkage of the lattice. This may be favorable for the emergence of SC in terms of the wisdom of BCS theory. Moreover, compressing a topological material into a superconductor may also be beneficial to realize the so-called topological superconductivity where there exist so-called Majorana modes relevant to fault-tolerant quantum computations.

Recently, transition-metal dipnictide $PtBi_2$ stood out as a new system hosting extraordinary XMR effect.[16–23] Generally, the binary compound $PtBi_2$ has two structural polymorphs that are easily accessible in lab, i.e., three-dimensional cubic $PtBi_2$ with space group $Pa\bar{3}$ (No. 205) and distorted layered quasi-two-dimensonal trigonal $PtBi_2$ with space group $P31m$ (No. 157). Investigations show that cubic $PtBi_2$ is a Dirac semimetal[16,24] and trigonal $PtBi_2$ is a semimetal with unique triply degenerate point fermions,[17] the former of which even exhibits the highest MR observed among the known non-magnetic metals so far.[16] Just as told by the above empirical rule, compressing cubic $PtBi_2$ can suppress its XMR and turn it into a superconductor.[25] The pressure-induced SC in cubic $PtBi_2$ above ∼13 GPa has nothing to do with any structural anomalies and is related to pronounced enhancement in carriers density of both electrons and holes.

Here, we show that trigonal $PtBi_2$ becomes a superconductor upon compression inside a diamond anvil cell with pressures above ∼5-6 GPa. While no evident trace of structural transitions is observed, the emergence of SC in trigonal $PtBi_2$ may be related to a positive-to-negative sign change of the Hall coefficient.

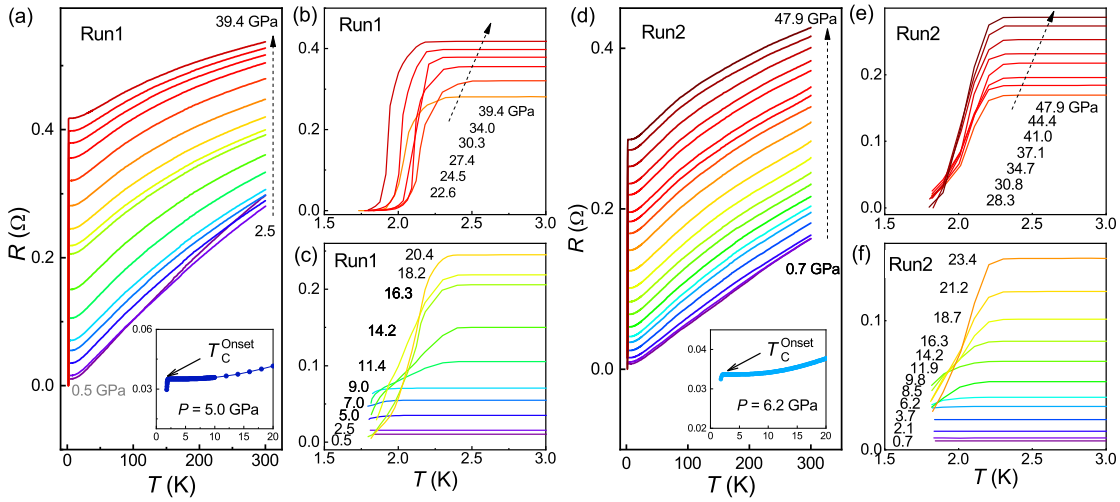

FIG. 1. (a) Pressure dependence of *dc* electric resistance (R) of trigonal $PtBi_2$ in the temperature range of 1.8-300 K (Run1). Inset: Low temperature R at 5.0 GPa. T_C^{Onset} is defined as the onset temperature of resistance drop in $R-T$. (b) and (c) are enlarged views of low-temperature resistance in Run1. (d) High-pressure electrical transport measurements in a second run (Run2). (e) and (f) are enlarged views of low-temperature resistance in Run2.

II. EXPERIMENTAL DETAILS

The grown method of single crystals can be found elsewhere.[17] High-pressure resistance and Hall effect measurements were performed by using an in-house multifunctional physical properties measurement system (temperature: 1.8-300 K; magnetic field: 0-±9 T). The preparation details of samples inside the diamond anvil cells (DACs) and data processing procedures for the above transport experiments are almost the same as those in a previous report.[25]

The room-temperature angle-dispersive synchrotron x-ray diffraction (XRD) experiments were carried out on a piece of single crystal ($\sim 50\times 50\times 5\ \mu m^3$), at the beamline 16 BM-D of HPCAT,[26] Advanced Photon Source, Argonne National Laboratory. The x-ray wavelength is 0.3100 Å. Daphne 7373 was employed as the pressure-transmitting medium. The DIOPTAS program[27] was used for image integrations. Pressure was determined by the ruby fluorescence method at room temperature.[28]

III. RESULTS AND DISCUSSION

Figure 1 shows the in-plane resistance (R) as a function of temperature at different applied pressures for two runs. In Fig. 1(a) (Run1), at 0.5 GPa trigonal $PtBi_2$ shows a metallic behavior in the temperature range of 1.8-300 K , similar to previous reports at ambient pressure.[17–19,21,23] Upon further compression, the $R-T$ curves shift upwards progressively. In addition, a tiny resistance drop begins to be observed at P_C=5.0 GPa, with an onset temperature of $T_C^{Onset}\sim 2.0$ K, see the inset of Fig. 1(a). Afterwards, the drop in resistance gets more and more evident with increasing pressure and zero resistance is observed above 22.6 GPa [see Figs. 1(b) and 1(c)], indicating that the resistance drop should be a superconducting phase transition. The T_C^{Onset} has a very weak pressure dependence, varying slightly within a temperature window of ±0.3 K. These observations in transport properties are well reproducible in another run [Run2, Figs. 1(d-f)]. Note that trigonal $PtBi_2$ does not show any sign of SC at ambient pressure with temperatures down to as low as 50 mK (not shown).

The resistive superconducting transition is further evidenced by measuring the magnetic field dependence of resistance at a fixed pressure of 22.6 GPa. As expected, one can see that the resistance drop shifts to lower temperatures gradually with increasing field and almost smears out above 3.0 kOe, as shown in Fig. 2(a). To estimate the upper critical field ($\mu_0 H_{C2}$), we choose a resistance criterion of $\rho_{cri}=90\%\rho_n$ (ρ_n is the normal state resistance just above T_C^{Onset}) and then plot the data in Fig. 2(b). The WHH model[29] was used to fit the data, which yields an estimated zero-temperature upper critical field $\mu_0 H_{C2}(0)$ of ∼7.7 kOe. This value is far below the BCS weak-coupling Pauli limit of $\sim 1.84\times T_C$ (36.8 kOe). We would like to mention that as *ac* susceptibility measurements under such high pressure and low temperature is very challenging, the susceptibility data is lacking at present. Therefore, we cannot rule out the possibility of filamentary superconductivity, leaving the question of bulk superconductivity in trigonal $PtBi_2$ under pressure open.

Trigonal $PtBi_2$ was reported to be a XMR material at ambient pressure.[17] Now we investigate the pres-

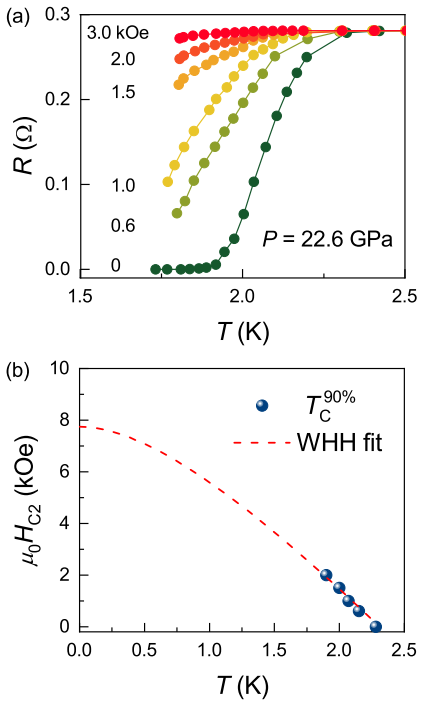

FIG. 2. (a) The resistive superconducting phase transition of trigonal $PtBi_2$ at 22.6 GPa in magnetic fields to 3.0 kOe. (b) Temperature dependence of the upper critical field $\mu_0 H_{C2}$. The red solid line is a fit to the data as described in the main text.

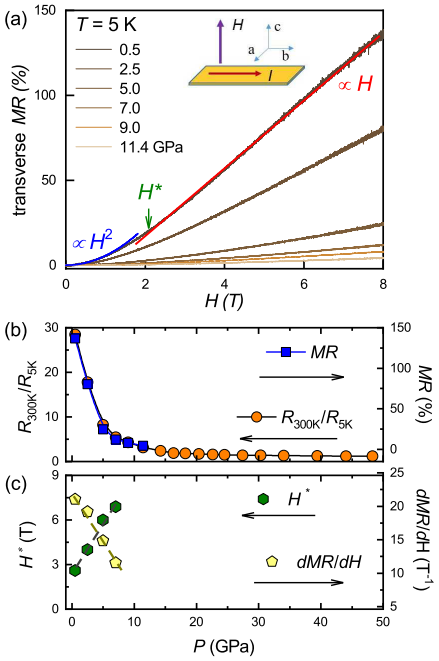

FIG. 3. (a) The transverse MR of trigonal $PtBi_2$ at 5 K under different pressures. Inset is a schematic of direction relationships of the applied current, the sample natural cleavage facet and the applied magnetic field. At low fields MR $\propto H^2$ while beyond H^* a linear field dependence is observed. (b) Plots of MR and $RRR = R_{300K}/R_{5K}$ versus pressure. (c) The crossover field $H^\star$ and the slope of the high-field linear MR as a function of pressure.

sure effect on its MR. With the application of external pressure, the transverse MR of trigonal $PtBi_2$ [MR=100%$\times(R(H) - R(0))/R(0)$] gets suppressed remarkably as seen from Fig. 3(a). For example, at 0.5 GPa the MR is about 135% compared to an ambient-pressure value of about 10000% at the same temperature and field conditions.[17] A previous study on the XMR effect in semimetals reveals that at a given condition the higher the residual resistivity ratio RRR value ($= R_{300K}/R_{5K}$) is and thereby the better the sample quality is, the higher the XMR value is.[30] This is applicable for the present case as the RRR value changes from ∼800 at ambient pressure[17] to ∼29, say at 0.5 GPa. In addition, such great suppression of MR has also been observed in other XMR semimetals with extremely high carriers mobility and may be likely due to rapid decrease in carriers mobility (μ).[7,25] In the present case, the rapid decrease in MR may be related to a change of carriers density itself as indicated by the Hall measurements below. From Fig. 3(b), we find that the transverse MR (at 5 K and 8 T) scales well with the residual resistance ratio RRR, suggesting a close relationship between the MR and the RRR as also reported before.[23] The shape of the transverse MR versus H can be divided by a crossover field $H^\star$ into two regions: the MR below $H^\star$ shows a quadratic field dependence, whereas it increases linearly above $H^\star$. One can see that dMR/dH changes almost inversely with $H^\star$ [Fig. 3(c)], which may imply a classical disorder mechanism for the linear MR.[18]

To check whether the pressure-induced superconductivity links to a structural transition or not, we performed high-pressure synchrotron XRD experiments at room temperature. We found that trigonal $PtBi_2$ is unstable if being ground in the air. As such, we collected the XRD data directly by using a Mao-Bell type diamond anvil cell with a piece of freshly cleaved single crystal inside. Representative raw diffraction images at 2.1, 6.9 and 12.9 GPa are displayed in the left column of Fig. 4. Clearly, spots with six-fold rotational symmetry can be observed. The integrated intensity versus 2theta patterns are shown in the middle column of Fig. 4. Starting at 2.1 GPa, all the peaks except for two minor ones marked by star (from cubic phase) can be indexed by the trigonal structure with space group $P31m$ (No. 157). With increasing pressure, the XRD peaks shift to higher angles due to shrinkage of the lattice. No evident changes or new peaks can be discerned to 12.9 GPa, suggesting a stable lattice structure of trigonal $PtBi_2$ in this pressure range. The extracted lattice parameters by using the RIETICA program[31] with the Le Bail method and the equation of state (EOS) are displayed in the right column of Fig. 4. The EOS is fitted by the third-order Birch-Murnaghan equation,[32] which gives the unit-cell volume $V_0 = 230.2$

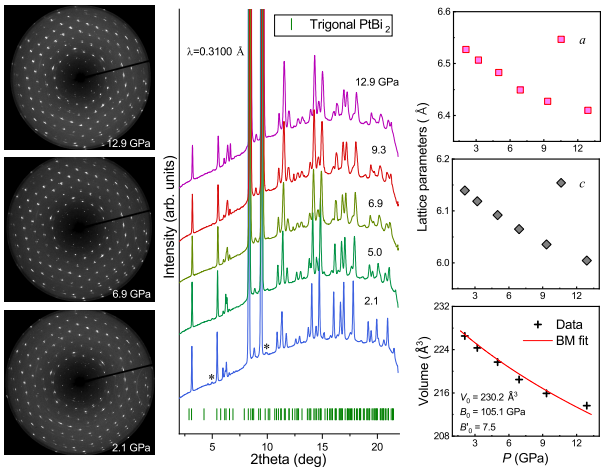

FIG. 4. Left column: representative experimental raw images at 2.1, 6.9, 12.9 GPa. Middle column: XRD patterns at various pressures. The synchrotron x-ray wavelength is λ=0.3100 Å. Peaks marked with star are from the cubic phase of $PtBi_2$. Right column: lattice parameters and the volume as a function of pressure (equation of state, EOS). The EOS data is fitted by the third-order Birch-Murnaghan formula.

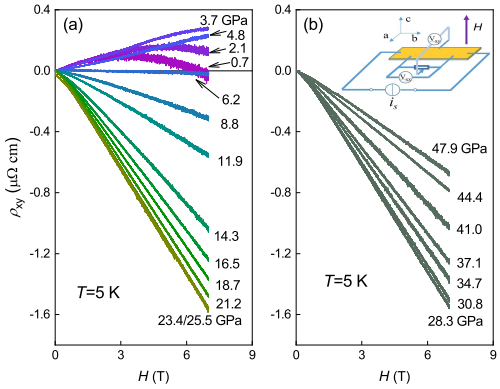

FIG. 5. Hall resistivity as a function of field ($\rho_{xy}(H)$) at different pressures and a fixed temperature of 5 K. Inset of (b) shows a schematic setup of the Hall effect measurement.

Å^3, the bulk modulus $B_0 = 105.1$ GPa and its first-order derivative $B_0^{'} = 7.5$.

Next we checked the carriers information of trigonal $PtBi_2$ under high pressure via Hall effect measurements. In Fig. 5, we show the field dependence of Hall resistivity [$\rho_{xy}(H)$] at various pressures and a fixed temperature of 5 K. Starting at 0.7 GPa, the positive $\rho_{xy}(H)$ first increases at low fields and then turns to decrease at higher fields, followed by a trend to change its sign to negative. This observation is similar to the previous reports at ambient pressure,[17,19,23] which is a characteristic of multiple bands crossing the Fermi level. With increasing pressure, the high-field down turn becomes less and less evident and almost a linear behavior of $\rho_{xy}(H)$ is

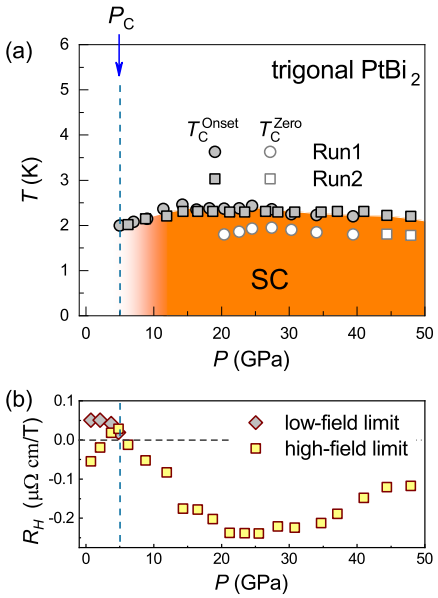

FIG. 6. (a) Temperature-pressure phase diagram of trigonal $PtBi_2$. P_C indicates the critical pressure where superconductivity is initially observed. (b) Hall coefficient (R_H) determined from the low-field or high-field limits of $\rho_{xy}(H)$.

observed. From 4.8 to 6.2 GPa, the slope of the linear $\rho_{xy}(H)$ changes its sign from positive to negative, indicating a crossover of the dominant carriers type. We note that this pressure coincides with the critical one where SC is initially observed [Run2, Fig. 1(d)], implying an intimate relationship between them. When the pressure is further increased, the magnitude of the negative slope of $\rho_{xy}(H)$ increases gradually and then decreases again after reaching a maximum at 23-25 GPa. Such magnitude fluctuations may indicate that the multiband character of trigonal $PtBi_2$ remains under high pressure.

We plot the Hall coefficient R_H at the field limits and the superconducting phase diagram of trigonal $PtBi_2$ together in Fig. 6. It can be readily seen that above the critical pressure P_C ~5-6 GPa, SC emerges and the low-field limit of R_H changes its sign from positive to negative simultaneously. At the same time, the negative high-field limit of R_H crosses the zero horizon line and reach a local positive maximum. These results imply that while the concentration of the hole-type carrier increases upon initial compression, the emergence of SC should be triggered by rapidly enhancement in concentration of the electron-type carrier.

Finally, we would like to compare the high-pressure results obtained for $PtBi_2$ between the cubic and the trigonal phases. In cubic $PtBi_2$, SC occurs above P_C ~13 GPa with no structural transition.[25] In addition, the superconducting transition temperature is ~2.2 K and is pressure insensitive. These observations are similar to those of trigonal $PtBi_2$ except for the P_C (~5-6 GPa). The most significant difference between the two cases is from the Hall response when SC occurs. For cubic $PtBi_2$,

it is always of carriers compensation at high pressures.[25] The occurrence of SC is related to simultaneous enhancements of both the electrons and holes concentrations. In contrast, trigonal $PtBi_2$ is not carriers compensated.[17,23] The emergence of SC may be related to a sign crossover of the Hall coefficient from positive to negative, i.e., dominantly owing to enrichment in concentration of the electrons. Such differences may reflect their differences in lattice structure and electronic band topology.

IV. CONCLUSIONS

In summary, we have studied the high-pressure properties of trigonal $PtBi_2$ through a combination of electrical resistance, synchrotron XRD and Hall effect measurements. Our data evidences a pressure-induced SC in trigonal $PtBi_2$, which does not link to a structural transition but may be related to a positive-to-negative sign change of the Hall coefficient. The present study demonstrates again that it may be a good route to explore SC by compressing the XMR materials. In addition, since SC in $PtBi_2$ under pressure is related to a change in carriers density, doping are expected to be effective in inducing SC in the system.

ACKNOWLEDGMENTS

The authors are grateful for the financial support from the National Key Research and Development Program of China (Grant Nos. 2016YFA0401804 and 2018YFA0305704), the National Natural Science Foundation of China (Grant Nos. 11804344, U19A2093, U1632275, U1932152, 11874362, 11704387, 11804341, and U1832209), the Natural Science Foundation of Anhui Province (Grant Nos. 1808085MA06, 1908085QA18 and 2008085QA40), the Users with Excellence Program of Hefei Center CAS (Grant No. 2020HSC-UE015), and the Collaborative Innovation Program of Hefei Science Center CAS (Grant No. 2020HSC-CIP014). A portion of this work was supported by the High Magnetic Field Laboratory of Anhui Province under Contract No. AHHM-FX-2020-02. Yonghui Zhou was supported by the Youth Innovation Promotion Association CAS (Grant No. 2020443). We thank Changyong Park for supporting our XRD experiments. The X-ray experiments were performed at HPCAT (Sector 16), Advanced Photon Source, Argonne National Laboratory. HPCAT operations are supported by DOE-NNSAs Office of Experimental Sciences. The Advanced Photon Source is a U.S. Department of Energy (DOE) Office of Science User Facility operated for the DOE Office of Science by Argonne National Laboratory under Contract No. DE-AC02-06CH11357.

* Corresponding author: xlchen@hmfl.ac.cn
† Corresponding author: zryang@issp.ac.cn

[1] C. Buzea and K. Robbie, Assembling the puzzle of superconducting elements: a review, Supercond. Sci. Technol. **18**, R1 (2005).
[2] J. J. Hamlin, Superconductivity in the metallic elements at high pressures, Physica C: Superconductivity and its Applications **514**, 59 (2015).
[3] A. P. Drozdov, M. I. Eremets, I. A. Troyan, V. Ksenofontov, and S. I. Shylin, Conventional superconductivity at 203 kelvin at high pressures in the sulfur hydride system, Nature **525**, 73 (2015).
[4] M. Somayazulu, M. Ahart, A. K. Mishra, Z. M. Geballe, M. Baldini, Y. Meng, V. V. Struzhkin, and R. J. Hemley, Evidence for Superconductivity above 260 K in Lanthanum Superhydride at Megabar Pressures, Phys. Rev. Lett. **122**, 027001 (2019).
[5] M. R. Norman, The Challenge of Unconventional Superconductivity, Science **332**, 196 (2011).
[6] S. Sachdev and B. Keimer, Quantum criticality, Physics Today **64**, 29 (2011).
[7] X.-C. Pan, X. L. Chen, H. M. Liu, Y. Q. Feng, Z. X. Wei, Y. H. Zhou, Z. C. Chi, L. Pi, F. Yen, F. Q. Song, X. G. Wan, Z. R. Yang, B. G.Wang, G. H.Wang, and Y. H. Zhang, Pressure-driven dome-shaped superconductivity and electronic structural evolution in tungsten ditelluride, Nat. Commun. **6**, 7805 (2015).
[8] D. F. Kang, Y. Z. Zhou, W. Yi, C. L. Yang, J. Guo, Y. G. Shi, S. Zhang, Z. Wang, C. Zhang, S. Jiang, A. G. Li, K. Yang, Q. Wu, G. M. Zhang, L. L. Sun, and Z. X. Zhao, Superconductivity emerging from a suppressed large magnetoresistant state in tungsten ditelluride, Nat. Commun. **6**, 7804 (2015).
[9] Y. P. Qi, P. G. Naumov, M. N. Ali, C. R. Rajamathi,W. Schnelle, O. Barkalov,M. Hanfland, S.-C.Wu, C. Shekhar,Y. Sun,V. Süß, M. Schmidt, U. Schwarz, E. Pippel, P.Werner, R. Hillebrand, T. F¨rster, E. Kampert, S. Parkin, R. J. Cava, C. Felser, B. H. Yan, and S. A. Medvedev, Superconductivity in Weyl semimetal candidate $MoTe_2$, Nat. Commun. **7**, 11038 (2016).
[10] Y. H. Zhou, J. F. Wu, W. Ning, N. N. Li, Y. P. Du, X. L. Chen, R. R. Zhang, Z. H. Chi, X. F. Wang, X. D. Zhu, P. C. Lu, C. Ji, X. G. Wan, Z. R. Yang, J. Sun, W. G. Yang, M. L. Tian, Y. H. Zhang, and H.-K. Mao, Pressure-induced superconductivity in a three-dimensional topological material $ZrTe_5$, Proc. Natl. Acad. Sci. USA **113**, 2904 (2016).
[11] Y. Qi, W. Shi, P. G. Naumov, N. Kumar, W. Schnelle, O. Barkalov, C. Shekhar, H. Borrmann, C. Felser, B. Yan, and S. A. Medvedev, Pressure-driven superconductivity in the transition-metal pentatelluride $HfTe_5$, Phys. Rev. B **94**, 054517 (2016).
[12] Y. Liu, Y. J. Long, L. X. Zhao, S. M. Nie, S. J. Zhang, Y. X. Weng, M. L. Jin, W. M. Li, Q. Q. Liu, Y. W. Long, R. C. Yu, C. Z. Gu, F. Sun, W. G. Yang, H. K. Mao, X. L.

Feng, Q. Li, W. T. Zheng, H. M. Weng, X. Dai, Z. Fang, G. F. Chen, and C. Q. Jin, Superconductivity in $HfTe_5$ across weak to strong topological insulator transition induced via pressures, Sci. Rep. **7**, 44367 (2017).

[13] L. P. He, Y. T. Jia, S. J. Zhang, X. C. Hong, C. Q. Jin, and S. Y. Li, Pressure-induced superconductivity in the three-dimensional topological Dirac semimetal Cd_3As_2, npj Quantum Mater. **1**, 16014 (2016).

[14] Y. Luo, H. Li, Y. M. Dai, H. Miao, Y. G. Shi, H. Ding, A. J. Taylor, D. A. Yarotski R. P. Prasankumar, and J. D. Thompson, Hall effect in the extremely large magnetoresistance semimetal WTe_2, Appl. Phys. Lett. **107**, 182411 (2015).

[15] T. Liang, Q. Gibson, M. N. Ali, M. Liu, R. J. Cava, and N. P. Ong, Ultrahigh mobility and giant magnetoresistance in the Dirac semimetal Cd_3As_2, Nat. Mat. **14**, 280 (2014).

[16] W. S. Gao, N. N. Hao. F.-W. Zheng, W. Ning, M. Wu, X. D. Zhu, G. L. Zheng, J. L. Zhang, J. W. Lu, H. W. Zhang, C. Y. Xi, J. Y. Yang, F. F. Du, P. Zhang, Y. H. Zhang, and M. L. Tian, Extremely Large Magnetoresistance in a Topological Semimetal Candidate Pyrite $PtBi_2$, Phys. Rev. Lett. **118**, 256601 (2017).

[17] W. S. Gao, X. D. Zhu, F. W. Zheng, M. Wu, J. L. Zhang, C. Y. Xi, P. Zhang, Y. H. Zhang, N. Hao, W. Ning, and M. L. Tian, A possible candidate for triply degenerate point fermions in trigonal layered $PtBi_2$, Nat. Commun. **9**, 3249 (2018).

[18] X. J. Yang, H. Bai, Z. Wang, Y. P. Li, Q. Chen, J. Chen, Y. K. Li, C. M. Feng, Y. Zheng, and Z.-A. Xu, Giant linear magneto-resistance in nonmagnetic $PtBi_2$, Appl. Phys. Lett. **108**, 252401 (2016).

[19] C. Q. Xu, X. Z. Xing, X. F. Xu, B. Li, B. Chen, L. Q. Che, X. Lu, J. H. Dai, and Z. X. Shi, Synthesis, physical properties, and band structure of the layered bismuthide $PtBi_2$, Phys. Rev. B **94**, 165119 (2016).

[20] Q. Yao, Y. P. Du, X. J. Yang, Y. Zheng, D. F. Xu, X. H. Niu, X. P. Shen, H. F. Yang, P. Dudin, T. K. Kim, M . Hoesch, I. Vobornik, Z.-A. Xu, X. G. Wan, D. L. Feng, and D. W. Shen, Bulk and surface electronic structure of hexagonal structured $PtBi_2$ studied by angle-resolved photoemission spectroscopy, Phys. Rev. B **94**, 235140 (2016).

[21] B. L. Wu, V. Barrena, H. Suderow, and I. Guillamón, Huge linear magnetoresistance due to open orbits in γ-$PtBi_2$, Phys. Rev. Research **2**, 022042(R) (2020).

[22] S. Thirupathaiah, Y. Kushnirenko, E. Haubold, A. V. Fedorov, E. D. L. Rienks, T. K. Kim, A. N. Yaresko, C. G. F. Blum, S. Aswartham, B. Büchner, and S. V. Borisenko, Possible origin of linear magnetoresistance: Observation of Dirac surface states in layered $PtBi_2$, Phys. Rev. B **97**, 035133 (2018).

[23] L. Y. Xing, R. Chapai, R. Nepal, and R. Y. Jin, Topological behavior and Zeeman splitting in trigonal $PtBi_{2-x}$ single crystals, npj Quantum Materials **5**, 10 (2020).

[24] Q. D. Gibson, L. M. Schoop, L. Muechler, L. S. Xie, M. Hirschberger, N. P. Ong, R. Car, and R. J. Cava, Three-dimensional Dirac semimetals: Design principles and predictions of new materials, Phys. Rev. B **91**, 205128 (2015).

[25] X. L. Chen, D. X. Shao, C. C. Gu, Y. H. Zhou, C. An, Y. Zhou, X. D. Zhu, T. Chen, M. L. Tian, J. Sun, and Z. R. Yang, Pressure-induced multiband superconductivity in pyrite $PtBi_2$ with perfect electron-hole compensation, Phys. Rev. Materials **2**, 054203 (2018).

[26] C. Park, D. Popov, D. Ikuta, C. L. Lin, C. Kenney-Benson, E. Rod, A. Bommannavar, and G. Shen, New developments in micro-X-ray diffraction and X-ray absorption spectroscopy for high-pressure research at 16-BM-D at the Advanced Photon Source, Rev. Sci. Instrum. **86**, 072205 (2015).

[27] C. Prescher and V. B. Prakapenka, DIOPTAS: a program for reduction of two-dimensional X-ray diffraction data and data exploration, High Press. Res. **35**, 223 (2015).

[28] H. K. Mao, J. Xu, and P. M. Bell, Calibration of the ruby pressure gauge to 800 kbar under quasi-hydrostatic conditions, J. Geophys. Res. **91**, 4673 (1986).

[29] N. R. Werthamer, E. Helfand, and P. C. Hohenberg, Temperature and Purity Dependence of the Superconducting Critical Field, H_{C2}. III. Electron Spin and Spin-Orbit Effects, Phys. Rev. **147**, 295 (1966).

[30] M. N. Ali, L. Sshoop, J. Xiong, S. Flynn, Q. Gibson M. Hirschberger, N. P. Ong, and R. J. Cava, Correlation of crystal quality and extreme magnetoresistance of WTe_2, EPL **110**, 67002 (2015).

[31] B. A. Hunter, RIETICAA Visual Rietveld Program, International Union of Crystallography Commission on Powder Diffraction, Newsletter No. 20 (Summer1998). http://www.rietica.org.

[32] F. Birch, Finite elastic strain of cubic crystals, Phys. Rev. **71**, 8093 (1947).